

Fig.A5.1-8 Local bond stress-slip relationship for NSM FRP in case of epoxy cover splitting failure

In general, the ultimate slips of bond laws in NSM systems are higher than the respective ones in EBR systems. Test results on bond tests carried out on different NSM systems have evidenced that the local bond-slip law can also be reasonably approximated by a bilinear diagram, as in Fig.5-1, with parameters depending on the axial stiffness, the shape and the surface treatment¹⁵.

The ultimate slip can increase with the roughness of the surface of the FRP, resulting in an increase of the energy absorption capacity. Both the peak shear stress τ_{b1} and the ultimate slip s_0 increase with the decrease of the axial stiffness of the FRP; and the elastic stiffness of the bond law increases as the axial stiffness of the FRP increases.

The surface treatment is expected to be reflected both on the peak value of the shear stress and on the post-peak behaviour: a rougher surface should increase the peak stress and the post-peak behaviour is, in general, more brittle in case of a smooth surface, due to the rapid decay of bond, since the interlocking phenomena are less pronounced.

The ability of most types of NSM FRP reinforcement to transfer shear stresses to the concrete for large relative displacements results in high values of fracture energy G . Hence, unlike for EBR systems, for NSM reinforcement it is generally possible to transfer forces up to the ultimate tensile strength of the FRP materials over a relatively small bond length at a single crack (for bond lengths in the range 150 mm to 200 mm, depending on the elastic modulus of the adhesive).

A5.1.2.2 Database on design by testing for assessing the maximum strain at failure in NSM FRP

An empirical formulation for calculating the maximum strain in the NSM FRP reinforcement is proposed by one study⁸⁴, based on the statistical regression of data from bond tests. A database of 174 test results has been selected, corresponding to different types of bond failure: epoxy-concrete interface failure, epoxy-FRP interface failure, and epoxy splitting. The maximum strain depends on the perimeter of the groove, p_g the elastic modulus E_f and the area A_f of the FRP, according to the following expression:

$$\varepsilon_{\max,th} = a \frac{\left(\frac{p_g}{E_f \cdot A_f}\right)^c}{(A_f)} \quad (\text{A5-14})$$

In case of mean value provision the regression coefficients a,b and c are 252,0.823 and 0.66, respectively, corresponding to $R^2=0.82$. For the 5% characteristic values the coefficient a becomes 157.

The mean and characteristic provisions given by Eq.(A5-14) are compared with the experimental database of 174 results used for the assessment of the numerical coefficients in Fig.A5.1-9.

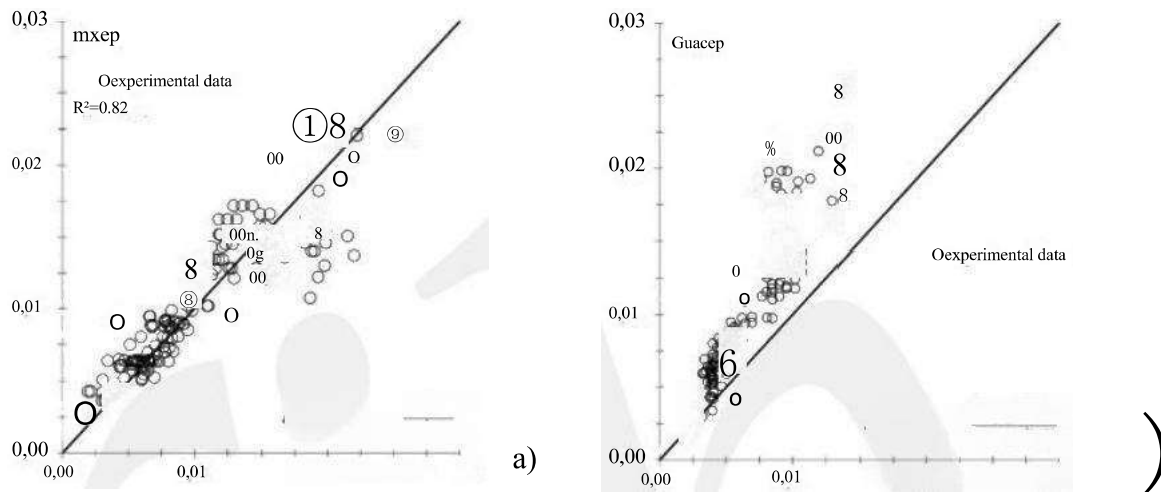


Fig.A5.1-9 Experimental maximum strain versus theoretical values given by Eq.(A5-14):(a)mean values; (b)characteristic values84

Appendix 5.2-Special types of strengthening systems

A5.2.1 Textile reinforced mortar (TRM) reinforcement

Textile reinforced mortar (TRM) composites are described in Section 2.3.2.9. As in case of FRP composites, RC elements strengthened with TRM are reported to fail due to debonding. Whereas in FRP-strengthened elements debonding occurs within a thin layer of concrete, the weakness of TRM-concrete joints has in many cases been reported to be at the matrix-fibre interface, with failure characterised by increasing slippage of the fibre bundles with respect to the surrounding matrix^{93,94,95}. The behaviour of the composite is strongly influenced by the matrix-fibre interfacial bond, which in turn is affected by the capacity of the matrix to penetrate within the bundles impregnating single fibre filaments⁹⁶. The bond behaviour of TRM-concrete joints can be investigated through direct-shear tests. Some results obtained with single-lap direct-shear tests showed that an effective bond length, i.e. the minimum length needed to fully establish the stress-transfer mechanism, can be defined. Nevertheless, the bond behaviour of TRM-concrete joints is complicated by the presence of friction (interlocking) between single fibre filaments, which always occurs when the textile is loaded, and between matrix and fibre for the portion of textile debonded⁹⁷. The presence of friction affects the peak load of TRM-concrete joints determining an increase of the applied load beyond the joint load-carrying capacity.

Several different types of TRM composites, which may comprise carbon, glass, basalt or other types of fibres, are currently available. They can be applied to the properly treated concrete substrate (e.g. by mechanical grinding, grind blasting, etc.) through different types of mortar matrices. In addition, the fibre bundles can be coated to improve the

matrix-fibre bond behaviour. All these elements affect the bond properties and in turn may determine a different behaviour of the strengthened element. Further investigations, possibly with improved test set-ups, are needed to have a deeper knowledge of the TRM-concrete bond.

A5.2.2 Steel fibre reinforced polymer (SFRP)reinforcement

When using steel fibre reinforced polymers(SFRP)as external reinforcement, the required anchorage length and transferable anchorage force must be established, e.g. through modelling approaches such as the ones described in this chapter. The difference between the resulting equations and those presented above will be mainly in the calibration coefficients. Test results from two studies^{98,99} indicate that the effective bond length is somewhat larger when SFRP materials are used instead of traditional FRP.

A5.2.3 Mechanically anchored or fastened systems

Mechanically anchored(anchors in addition to the adhesive bonding)or fastened(entirely mechanically attached)FRP is described in Section 2.3.2.7. As far as bond behaviour is concerned, the mechanics and specific modelling approaches depend heavily on the type, quantity, spacing and arrangement of the fasteners.

6. Ultimate limit states for predominantly static loading and fatigue

6.1 General

This chapter presents guidelines for the verification of the ultimate limit states for reinforced or prestressed concrete members subjected to predominantly static loading and fatigue. It covers mainly bending with or without axial force (strengthening of beams for bending, strengthening of columns for predominantly axial load through confinement and strengthening of columns for bending with axial force), shear, torsion and fatigue. Punching, design with strut and tie models, anchorages and laps are briefly discussed too.

6.2 Bending with or without axial force

6.2.1 Strengthening with externally bonded FRP for members subjected primarily to bending

6.2.1.1 Basic principles and failure modes

Reinforced concrete elements, such as beams, slabs and columns, may be strengthened in flexure through the use of FRP epoxy-bonded to their tension zones (Fig. 6-1), with the direction of fibres parallel to that of high tensile stresses.

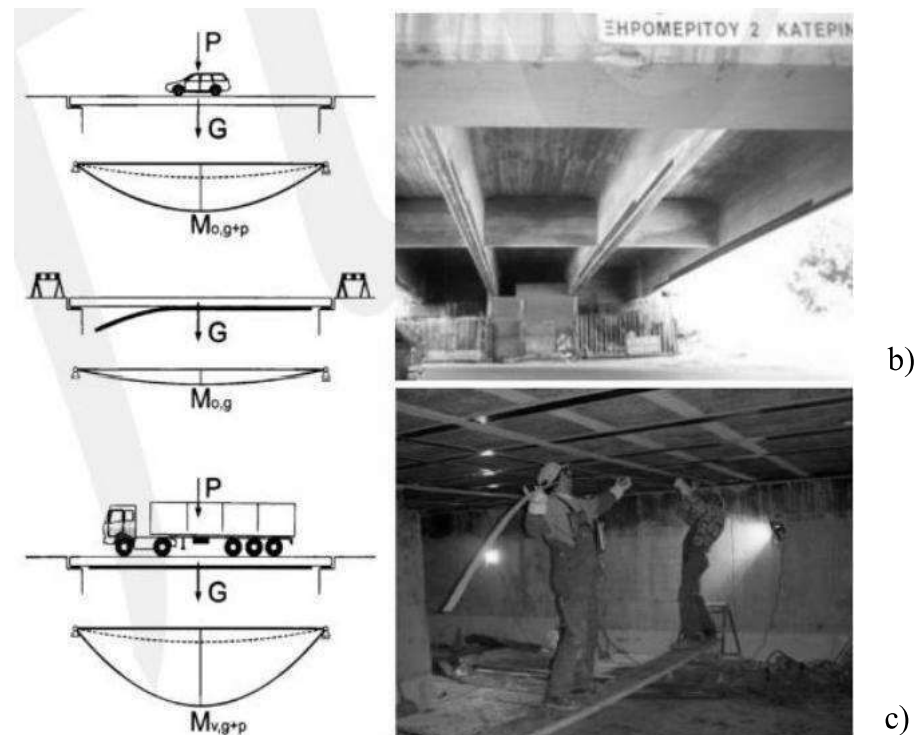


Fig. 6-1 Flexural strengthening: (a) bridge, (b) RC beams and (c) RC slab with FRP strips

This chapter was mainly authored by Matthys and Triantafillou.

In Fig.6-1,a typical loading situation is illustrated before(Fig.6-1a,top),during (Fig.6-1a,middle)and after(Fig.6-1a,bottom figure)flexural strengthening.Typical load-deflection curves for an unstrengthened and three strengthened RC beams are compared in Fig.6-2.An increase in the stiffness of the cracked beam can be noted,depending on the amount of axial stiffness added to the beam through the FRP.The increased stiffness limits deflections at service load level.In terms of cracking,typically more yet smaller cracks will be observed for the strengthened beam.The yield moment is slightly increased.A considerable increase in the load bearing capacity is obtained through the additional FRP reinforcement,at the expense of a reduction of the ultimate deflection at which the strengthened beam fails.The failure mode often tends to be of brittle nature, and may typically correspond to debonding between the FRP and the concrete.

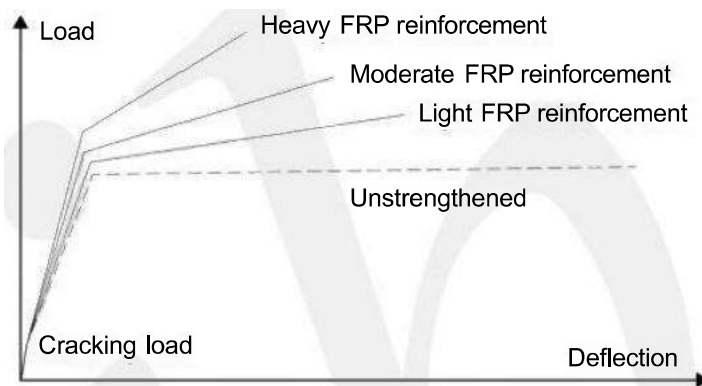


Fig.6-2 Load-deflection curves for different degrees of flexural strengthening

The analysis for the ultimate limit state for such elements may follow well-established procedures for reinforced concrete structures, provided that:(a)the contribution of external FRP reinforcement is taken into account properly; and (b)special consideration is given to the issue of bond between the concrete and the external reinforcement.

The following assumptions are made:

- The slip between the FRP and the substrate is negligible. This assumption is justified for most high quality structural adhesives applied with a thickness in the order of 1.0 mm,in which case viscoelastic phenomena,such as axial and shear creep as well as relaxation,are negligible.
- Interlaminar shear strength of the FRP is higher than the adhesive bond shear strength; this can be covered by specifying the proper resins.
- The surface preparation of the concrete substrate is sufficient to achieve the level of bond strength required in the design.
- The strain state of the existing reinforcement at the time of strengthening(initial situation)may be determined on the basis of elastic analysis of the cracked cross section.

A concrete beam strengthened in flexure with externally applied FRP may fail according to the following failure modes1,2,3:

- Steel yielding followed by concrete crushing
- Steel yielding followed by FRP rupture

- Concrete crushing(this brittle failure mode is not permitted)
- Loss of composite action due to debonding,typically after (and rarely before) steel yielding;this is the most prevalent failure mode

In cases where the FRP will reach its design tensile strain before the concrete crushes, failure normally occurs due to debonding rather than rupture.Debonding occurs through the concrete,which is the "weak link" in terms of bond capacity,according to one of the following three failure modes (also discussed in Section 5.2.1):

- Intermediate crack debonding(Fig.6-3a)
- End debonding(interfacial failure of end anchorage)(Fig.6-3b)
- Concrete cover separation(rip-off failure of end anchorage)(Fig.6-3c)

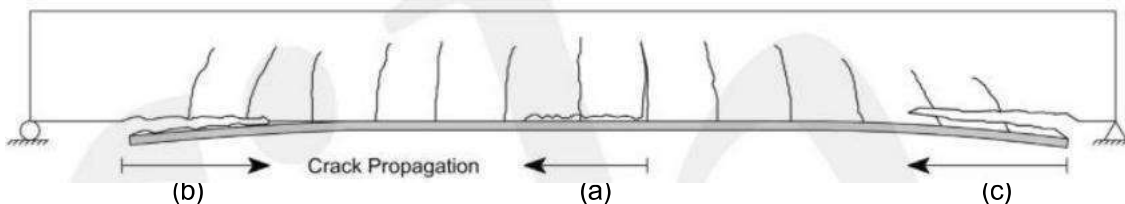


Fig.6-3 Debonding failure modes of a concrete member with externally bonded FRP:(a)Intermediate crack debonding;(b)end debonding;(c)concrete cover separation

As described in Chapter 5,intermediate crack debonding and end debonding develop when the bond strength is exceeded and they are different only with respect to the starting point of the debonding process.The behaviour of bond between FRP and concrete and hence both intermediate crack debonding and end debonding can be characterised on the basis of the bond shear stress-shear slip relation.

Concrete cover separation develops when a shear crack in the end region of the FRP propagates into a debonding mode at the level below the internal steel reinforcement. The provisions for concrete cover separation are therefore listed in Section 6.3.5.1,as part of the shear verifications.

6.2.1.2 Analysis of flexural capacity

At each cross section of the strengthened member,it shall be ensured that the design resistance of the member is higher than the design value following from the applied load.Herby,the flexural capacity of the strengthened member is assessed by means of traditional cross-sectional analysis,on the basis of strain compatibility assuming full composite action between the FRP and the concrete substrate,horizontal equilibrium of forces and moment equilibrium.The load level during strengthening is taken into account through the acting strains in the cross section at the moment of EAR application. Provisions are given in Appendix 6.1.

Furthermore,the analysis will verify FRP debonding.Design provisions for intermediate crack debonding,end debonding and concrete cover separation are given in Sections 6.2.1.3, 6.2.1.4 and 6.3.5.2,respectively.For all these analyses the member shall be assumed to be fully cracked in the ultimate limit state,unless stated otherwise.

Following the proof of flexural load-bearing capacity, an analysis of the shear resistance (Section 6.3) shall be furnished. This to guarantee that shear failure does not become predominant after flexural strengthening and hence to verify if complementary shear strengthening is needed.

If the flexural strengthening is to be designed for predominantly non-static actions, a fatigue analysis according to Section 6.8 shall be conducted.

6.2.1.3 Intermediate crack debonding

Considering different levels of approximation, a simplified FRP stress limit method and a more accurate method are available for the analysis of intermediate crack debonding. The simplified FRP stress limit method is based on the ultimate FRP strain that has been defined on the safe side. This method can be rather conservative, as these simplified cut-off strains are generally lower than those predicted by more detailed calculations, given the different levels of approximation. The more accurate method is based on determining the crack spacing and on checking the FRP force difference at an element between two adjacent cracks.

The methods presented in this section account basically for flexural crack bridging, and not for flexural-shear crack bridging as discussed in Section 5.2.1.2(Fig.5-6b). Therefore, the provision of Section 6.3.5.2 should be additionally applied.

6.2.1.3.1 Simplified FRP stress limit method

The analysis of flexural strengthening for non-prestressed members may be simplified as analysis of flexural load-bearing capacity using the stress of the FRP in accordance with Eqs(5-14)-(5-16). In this approach an analysis of the bond force transmission at an element between cracks is not necessary. Yet, it assumes that proper end debonding detailing is done (Section 6.2.1.4).

The stress in the FRP at the ultimate limit state can be calculated as

$$\sigma_{id} = \min(f_{fibd,IC}, f_{id}) \quad (6-1)$$

where $f_{fibd,IC}$ = design value of the FRP bond strength corresponding to intermediate crack debonding, Eq.(5-16)(with $\beta_1=1$) or (6-2), and f = design tensile strength of FRP.

$$f_{fibd,IC} = \frac{k_{cr,k} \cdot k_k \cdot k_b \sqrt{\frac{2E_f}{t_f}} f_{cm}^{2/3}}{\gamma_{fb}} \quad (6-2)$$

All the parameters in Eq.(6-2) are defined in Sections 5.3.2.3 and 5.3.3.1 and are repeated here for the sake of convenience: $k_k=1.8$, $k_b=0.17$, $k_s=\sqrt{(2-b_e/b)/(1+b_e/b)}\geq 1$. Note that in Eq.(6-2) the elastic modulus of FRP E , and the concrete strength f_{cm} are in MPa; and the FRP thickness t_f is in mm.

6.2.1.3.2 More accurate method

The more accurate method comprises the verification of bond strength transmission at the elements between cracks. For this verification, it must be checked whether the change of the tensile force of the FRP, ΔF_d is lower than the resistance, ΔF_{Rd} at each concrete element between cracks:

$$\Delta F_d \leq \Delta F_{Rd} \quad (6-3)$$

The increment of FRP tensile force at the element between cracks can be calculated from the difference of the FRP tensile forces at both cracks:

$$\Delta F_{ba} = F_a(x+s) - F_a(x) \quad (6-4)$$

where s is the crack spacing.

Then, either a detailed analysis of bond strength transmission at the elements between cracks or a somewhat simplified analysis may be performed, as given next⁴.

Both analysis types start with the prediction of the crack spacing s_r for reinforced concrete members, which can be determined as:

$$s_r = 1.51e \quad (6-5)$$

where l = transfer length of the reinforcing steel, equal to

$$l_{e,0} = \frac{M_{cr}}{z_s \cdot F_{bsm}} \quad (6-6)$$

where M = cracking moment, $z_s \approx 0.85h$ (h = total member height) and F_{bsm} = bond force per length. In reinforced concrete members, the cracking moment may be approximated as

$$M = k_n f_c m W e \quad (6-7)$$

where $k_n = (1.6-h/1000) \geq 1$, h in mm and W = section modulus of the uncracked concrete cross section (moment of inertia divided by distance of the extreme tensile fibre from the neutral axis). When determining M for T-beams, the effective flange width shall be taken into account. The bond force per length may be calculated as

$$F_{bsm} = \sum_{i=1}^n n_{s,i} \pi \cdot \phi_{s,i} \cdot f_{bsm} \quad (6-8)$$

where f_{bsm} = mean bond stress of the reinforcing steel, n = number of steel rebars with diameter ϕ . One bar with equivalent diameter equal to $\sqrt{2}\phi$, shall be used for double bars. Equation (6-8) is based on the assumption of uniform bond stress along the reinforcing bar, from the cracked section up to the midpoint between successive cracks. The mean bond stress f_{bsm} may be obtained as follows:

$$f_{bsm} = \begin{cases} 0.43 \kappa_{vb1} \cdot f_{cm}^{2/3} & \text{for ribbed bars} \\ 0.28 \kappa_{vb2} \sqrt{f_{cm}} & \text{for smooth bars} \end{cases} \quad (6-9)$$

The parameters K_1 and K_2 depend on the bond conditions and may be taken as $K_1 = K_{vb2} = 1.0$ for good bond conditions and $K_1 = 0.7$ and $K_2 = 0.5$ for medium bond conditions.

-Detailed analysis of the FRP force difference at an element between cracks

The bond resistance to FRP force difference at an element between cracks is obtained by Eq.(6-10), as the summation of three components (Fig.6-4): one from the basic value of the adhesive bond of the FRP, one as a result of the bond friction and one as a result of the member curvature⁴:

$$\Delta F_{frd} = \frac{\Delta F_{ik,B} + \Delta F_{ik,F} + \Delta F_{ik,C}}{\gamma_{fb}} \quad (6-10)$$

The term related to adhesive bond, $\Delta F_{A,B}$, can be determined by using a bilinear approach for the bond law and the following equation:

$$\Delta F_{fk,B} = \begin{cases} \Delta F_{fk,B}^G - \frac{\Delta F_{fk,B}^G - \Delta F_{fk,B}^D}{F_{fk,B}^D} F_{fEd} & \text{for } F_{fEd} \leq F_{fk,B}^D \\ \sqrt{b_f^2 \cdot \tau_{b1k} \cdot s_{0k} \cdot E_f \cdot t_f + F_{fEd}^2} - F_{fEd} & \text{for } F_{fk,B}^D < F_{fEd} \leq F_{fd} \end{cases} \quad (6-11)$$

where b_f =width of FRP, F_d =FRP tensile load at the lower stressed crack, F_d =design breaking force of FRP strip,

$$\Delta F_{fk,B}^G = f_{fbk}(s_r) b_f \cdot t_f \quad (6-12)$$

$$\Delta F_{fk,B}^D = \sqrt{b_f^2 \cdot \tau_{b1k} \cdot s_{0k} \cdot E_f \cdot t_f + F_{fEd}^{D,2}} - F_{fEd}^D \quad (6-13)$$

$$F_{fk,B}^D = \frac{s_{0k} \cdot E_f \cdot b_f \cdot t_f}{s_r} - \tau_{b1k} \frac{s_r \cdot b_f}{4} \quad (6-14)$$

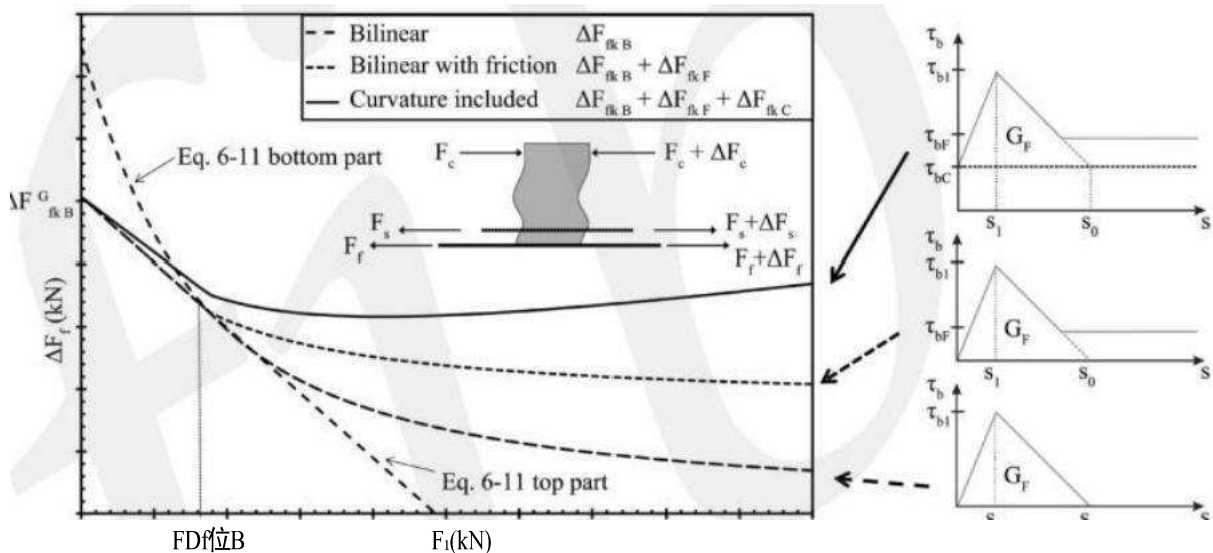


Fig.6-4FRP force due to basic bond,bond friction and member curvature⁴

The characteristic FRP bond strength $f_{fbk}(s)$ as a function of crack spacing is calculated according to Eq.(5-10) with $l_e=s$, and $\beta_1(s)$ calculated according to Eq.(5-9) with $/$ given by Eq.(5-3a):

$$f_{fbk}(s_r) = \begin{cases} \sqrt{\frac{E_f \cdot s_{0k} \cdot \tau_{b1k}}{t_f}} \frac{s_r}{l_e} \left(2 - \frac{s_r}{l_e} \right) & \text{for } s_r < l_e \\ \sqrt{\frac{E_f \cdot s_{0k} \cdot \tau_{b1k}}{t_f}} & \text{for } s_r \geq l_e \end{cases} \quad (6-15)$$

$$l_e = \frac{\pi}{2} \sqrt{\frac{E_f \cdot t_f \cdot s_{0k}}{\tau_{b1k}}} \quad (6-16)$$

The characteristic values of the shear strength t_k and the ultimate slip so can be taken from Table A5.1-15.

The share of the bond friction, $\Delta F_{fk,f}$, can be determined by Eq.(6-17):

$$\Delta F_{fk,f} = \begin{cases} 0 & \text{for } F_{fEd} \leq F_{fk,B}^D \\ \tau_{bfk} \cdot b_f \left[s_r - \frac{2t_f \cdot E_f}{\tau_{blk}} \left(\sqrt{\frac{\tau_{blk} \cdot s_{0k}}{E_f \cdot t_f} + \frac{F_{fEd}^2}{b_f^2 \cdot t_f^2 \cdot E_f^2}} - \frac{F_{fEd}}{b_f \cdot t_f \cdot E_f} \right) \right] & \text{for } F_{fk,B}^D < F_{fEd} \leq F_{fd} \end{cases} \quad (6-17)$$

where $t_f F_k$ is the characteristic bond friction strength (see Fig.6-4) that can be expressed according to the following formulation4:

$$\tau_{bfk} = 10.8 \alpha_{cc} \cdot f_{cm}^{-0.89} \quad (6-18)$$

where the coefficient α (between 0.8-1.0) accounts for long-term loading effects. Note that Eq.(6-18) can be used also to calculate the mean value of the friction term in the FRP, T_{bm} , with 10.8 replaced by 17.5.

The contribution of the member curvature can be calculated with the following equation:

$$\Delta F_{fk,C} = s_r \cdot K_k \frac{\varepsilon_f - \varepsilon_c}{h} b_f \quad (6-19)$$

where ε_f =strain in the FRP reinforcement at the lower stressed crack, ε_c =concrete strain at the lower stressed crack, h =depth of the cross section and K =calibration factor⁶, taken equal to $24.3 \cdot 10^3 \text{ N/mm}$. Note that Eq.(6-19) can be used also to calculate the mean value ΔF_c with 24.3 replaced by 33.3.

-Simplified analysis of the FRP force difference at an element between cracks

The strain of the steel reinforcement due to the load when the strengthening is applied shall be taken into account in this analysis. The strain in the FRP must not exceed the minimum of 0.01 and f_E at any point. The elements between cracks start at the maximum moment and extend to the last crack which is closest to the point of zero moment.

The detailed model based on the envelope line of tensile stress has the disadvantage that it is dependent on the FRP stress at the lower stressed crack of the element between cracks. Because of this, the principle of superposition is no longer valid. But the model can also be simplified on the safe side by using the following equation for the bond resistance to FRP force difference per element between cracks:

$$\Delta F_{frd} = \frac{2.3 \tau_{blk} \sqrt{s_r} + 0.1 \tau_{bfk} \cdot s_r^{4/3} + \frac{K_h}{h} s_r^{1/3}}{\gamma_{fb}} b_f \quad (6-20)$$

where $K_h=2000$ or 0 for reinforced or prestressed concrete members, respectively, the crack spacing s_r is limited to 400 mm, h =member height in mm (the value used shall be greater than 100 mm) and b_f =width of FRP in mm. Note that Eq.(6-20) can be used also to calculate the mean value ΔF_R with $K_h=2739$ (or 0), 2.3 replaced by 1.84 and 0.1 replaced by 0.095.

By simplification, the FRP force $F(x)$ may be obtained as a function of the tensile stress of the steel reinforcement in the strengthened state, $\sigma_s(x)$, as follows:

$$F_{fd}(x) = \begin{cases} \frac{\Delta M_{Ed}(x)}{z_m} \frac{d_f \cdot E_f \cdot A_f}{d_f \cdot E_f \cdot A_f + d_s \cdot E_s \cdot A_s} & \text{for } \sigma_s(x) < f_{yd} \\ \frac{M_{Ed}(x)}{z_m} - A_s \cdot f_{yd} & \text{for } \sigma_s(x) = f_{yd} \end{cases} \quad (6-21)$$

where $\Delta M(x)$ = additional bending moment after strengthening = $M(x) - ME_0(x)$, $M(x)$ = bending moment after strengthening, $ME_0(x)$ = bending moment during strengthening (initial situation), d_f = effective depth of FRP, d_s = effective depth of steel reinforcement, A_f = cross sectional area of FRP, A_s = cross sectional area of steel reinforcement, E_s = elastic modulus of steel, f_d = design yield strength of steel reinforcement, $\sigma_s(x)$ = tensile stress of the steel reinforcement and z_m = weighted lever arm, estimated as follows:

$$z_m \approx 0.8 \frac{d_f \cdot E_f \cdot A_f + d_s \cdot E_s \cdot A_s}{E_f \cdot A_f + E_s \cdot A_s} \quad (6-22)$$

By way of simplification, the tensile stress of the steel reinforcement in the strengthened state can be obtained as follows:

$$\sigma_s(x) = \sigma_{s,0}(x) + \frac{\Delta M_{Ed}(x)}{z_m} \frac{d_s E_s}{d_f \cdot E_f \cdot A_f + d_s \cdot E_s \cdot A_s} \leq f_{yd} \quad (6-23)$$

where $\sigma_{s,0}(x)$ = tensile stress of the steel reinforcement during strengthening, approximated as follows:

$$\sigma_{s,0}(x) = \frac{M_{E,0}(x)}{z_s \cdot A_s} = \frac{M_{E,0}(x)}{0.85 d_s \cdot A_s} \leq f_{yd} \quad (6-24)$$

where z_s = lever arm of steel reinforcement.

6.2.1.3.3 Other methods

A drawback of the method presented in Section 6.2.1.3.2, apart from its complexity, is the relatively large uncertainty typically observed on the prediction of the crack spacing. Two additional, alternative approaches for intermediate crack debonding verifications are presented in Appendix A6.2 (based on the bending moment-shear force interaction diagram) and Appendix A6.3 (based on the force transfer between concrete and FRP, assuming a fully cracked state). These models follow similar principles as the more accurate model presented above, yet apply different levels of approximation.

6.2.1.4 End debonding analysis

Two types of end debonding are considered (Chapter 5): interfacial debonding at the anchorage zone and concrete cover separation.

The end debonding analysis for interfacial debonding can be conducted on the basis of the FRP anchorage capacity, the latter being determined according to the design by testing approach described in Section 5.3.2.3. In this section, considering different levels of approximation, two approaches are presented. In the first approach⁷, outlined in Section 6.2.1.4.1, the FRP curtailment point is determined following a similar methodology as for curtailment of internal steel reinforcement according to Eurocode 28.9. Hereby, a

fully cracked state is assumed and the position of flexural cracks is not explicitly taken into consideration. To the contrary, in the second approach⁴, the position of flexural cracks is considered, so that the end debonding analysis is conducted at the flexural crack closest to the point of zero moment, in accordance with Section 6.2.1.4.2, or at an arbitrary concrete element between cracks in accordance with Section 6.2.1.4.3.

The end debonding analysis for concrete cover separation is done in accordance with Section 6.3.5.

6.2.1.4.1 Curtailment of FRP assuming fully cracked state

The maximum distance a , from the support, at which the FRP may be applied without risk of debonding, may be calculated by equating the design maximum tensile stress transferable to the FRP [Eq. (5-13)] to the stress in the FRP at a distance $a_1 + l_6$ from the support under the design load acting on the strengthened member. A schematic representation is given in Fig. 6-5a. The point of curtailment is taken in the zone where the resisting tensile force of the internal steel reinforcement is sufficient to carry the acting moments, the curtailment point being controlled by the fact that the acting stress in the FRP at a distance l of the end point should be smaller than f . Note that the analysis should be on the basis of a shifted moment line, following Eurocode 28 (sections 9.2.1.3 for beams or 9.3.1.1 for slabs).

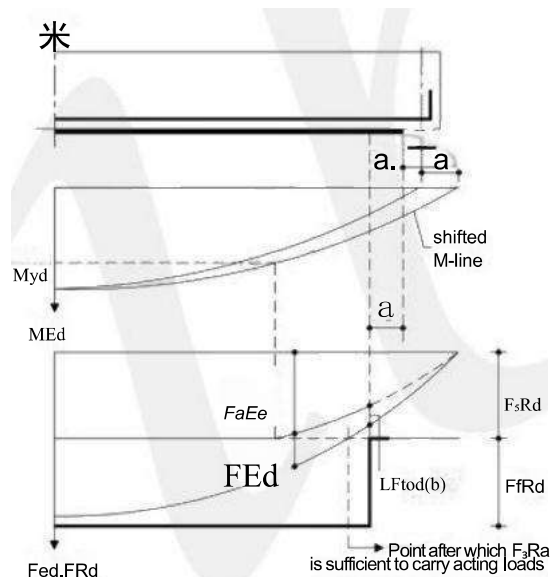


Fig. 6-5a Schematic representation of end debonding analysis, assuming a fully cracked state

In cases where the FRP is governed by the serviceability limit states of deflection or crack control, curtailment should consider that at least the complete cracked zone of the member is strengthened.

6.2.1.4.2 End anchorage at the flexural crack closest to the point of zero moment

The analysis at the flexural crack closest to the point of zero moment represents the standard case. This crack develops at the point where the bending moment equals the cracking moment M (Fig. 6-5b). The location of the flexural crack closest to the point of zero moment shall be obtained under the design loads in the ultimate limit state and without taking into account the shift of the tension envelope. Moreover, the prestrain of the reinforcement due to the load during strengthening shall not be taken into account in this analysis.

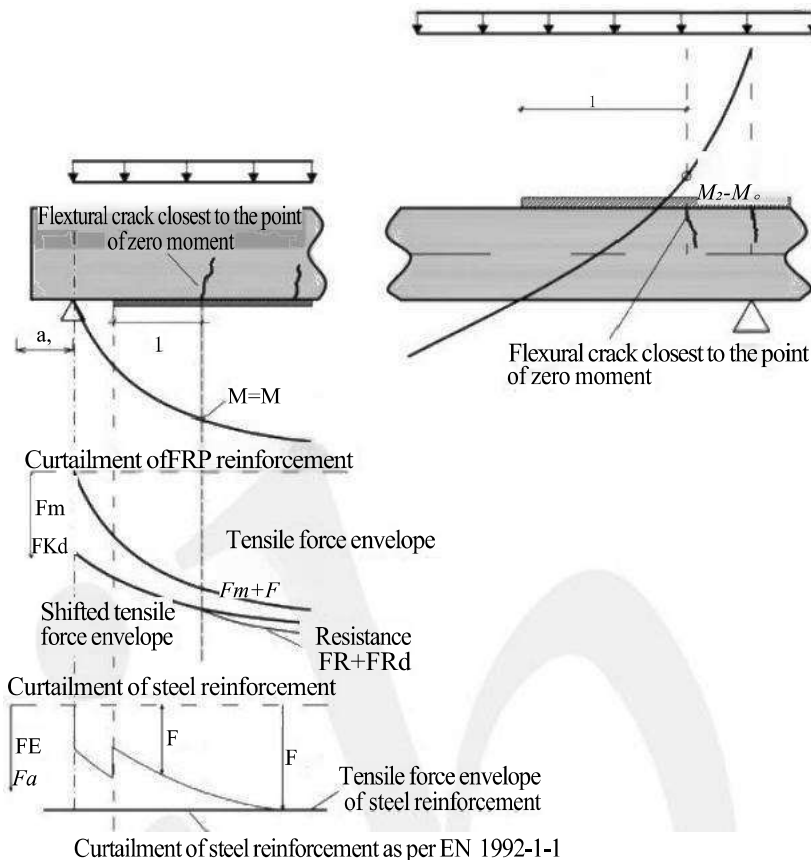


Fig.6-5b Schematic representation of end debonding analysis⁴

At the flexural crack closest to the point of zero moment, the applied moment M shall be smaller than the moment resistance $M_{Rd}(l_b)$, with the shift of the tension envelope taken into account according to Sections 9.2.1.3 for beams or 9.3.1.1 for slabs of EN 1992-1-18.

$$M_{Ed} \leq M_{Rd}(l_b) \quad (6-25)$$

The moment resistance shall be calculated through cross section analysis as a function of the strains $\varepsilon_{fRk}^a(l_b)$ in the FRP and $\varepsilon_{sRk}^a(l_b)$ in the steel reinforcement by means of Eq.(6-26), which considers a redistribution of stresses between the externally bonded and the internal reinforcement. The height of the compression zone and of the internal lever arms, z_a for the FRP and z_s for the steel reinforcement, may be determined through cross section analysis.

$$M_{Rd}(l_b) = \frac{\varepsilon_{fRk}^a(l_b) E_f}{\gamma_{fb}} A_f \cdot z_f^a + \frac{\varepsilon_{sRk}^a(l_b) E_s}{\gamma_s} A_s \cdot z_s^a \quad (6-26)$$

An example of cross section analysis for doubly reinforced rectangular cross sections is given in Appendix 6.1.

The strain of the FRP strip at the flexural crack closest to the point of zero moment is obtained as follows:

$$\varepsilon_{fRk}^a(l_b) = \begin{cases} \sin\left(\frac{\pi}{2} \frac{l_b}{l_{b,lim}}\right) \varepsilon_{fRk,lim} & \text{for } 0 < l_b < l_{b,lim} \\ \varepsilon_{fRk,lim} & \text{for } l_b \geq l_{b,lim} \end{cases} \quad (6-27)$$

where $\varepsilon_{frk,lim}^a$ can be estimated from the characteristic maximum bond strength of the FRP, f_{frk} , [Eq.(5-10) with $\beta_1=1$], as

$$\varepsilon_{frk,lim}^a \approx \frac{f_{frk}}{E_f} \quad (6-28)$$

and the corresponding anchorage length $l_{b,lim}$ can be obtained in terms of the maximum bond length l_b , [Eq.(5-7c)] as

$$l_{b,lim} \approx 0.9/l_b \quad (6-29)$$

The strain of the steel reinforcement is calculated as

$$\varepsilon_{sRk}^a(l_b) = K_{vb} \cdot K_{bsk} \left[s_r^a(l_b) \right]^{(a_n+1)/2} \left(\frac{d_s^a - x^a}{d_f^a - x^a} \right)^{(a_n+1)/2} \leq \frac{f_y k}{E_s} \quad (6-30)$$

where $a_n=0.25$ or 0 for ribbed or smooth steel reinforcement, respectively; $K=1$ or 0.7 for good or medium bond conditions, respectively; d =effective depth of steel reinforcement, d_f^a =effective depth of FRP reinforcement, x^a =depth of the compression zone and s_r^a =slippage of the FRP strip in mm, given as follows:

$$s_r^a(l_b) = \begin{cases} 0.213 \left[1 - \cos \left(\frac{\pi}{2} \frac{l_b}{l_{b,lim}} \right) \right] & \text{for } 0 < l_b < l_{b,lim} \\ 0.213 + (l_b - l_{b,lim}) \varepsilon_{frk,lim}^a & \text{for } l_b \geq l_{b,lim} \end{cases} \quad (6-31)$$

The bond coefficient for steel reinforcement K_{bsk} is obtained by means of Eq.(6-32). One bar with equivalent diameter equal to $\sqrt{2}\phi$ shall be used for double bars.

$$K_{bsk} = K_{b1k} \sqrt{\frac{f_{cm}^{K_{b2}}}{E_s \cdot \phi_s^{K_{b3}} (E_f \cdot t_f)^{K_{b4}}}} \quad (6-32)$$

where ϕ_s =largest steel diameter in mm, f_m , E_s and E_f in MPa and t in mm. The bond coefficients are $K_{b1k}=2.545$, $K_{b2}=1.0$, $K_{b3}=0.8$ and $K_{b4}=0.2$ for ribbed bars or $K_{b1k}=1.292$, $K_{b2}=1.3$, $K_{b3}=1.0$ and $K_{b4}=0.3$ for smooth bars.

6.2.1.4.3 End debonding analysis at an arbitrary concrete element between cracks

The second option-carrying out the end debonding analysis at an arbitrary element between cracks-may be necessary for those members in which owing to the low tensile strength of the concrete the flexural crack closest to the point of zero moment is close to the support. In this analysis the FRP has to be anchored at an arbitrary element between cracks similarly to the analysis according to Section 6.2.1.3.2. Besides taking into account the shift rule in this analysis, it has to be ensured that the cross section between the support and the element between cracks being considered possesses sufficient load-carrying capacity even without the FRP.

It shall be verified that at the element between cracks the acting FRP force F_d is lower than the resisting FRP force.

$$F_d \leq F_a \quad (6-33)$$

The resisting FRP force is obtained as follows:

$$F_{fibd} = b_f \cdot t_f \cdot f_{fibd}(s_r) \quad (6-34)$$

where the design bond strength as a function of the crack spacing, $f(s)$, is calculated from Eq.(5-13).

In calculating the acting FRP force, the initial strains in the cross section due to loads during strengthening may only be taken into account if the member is already in the cracked state at the end debonding analysis point prior to strengthening.

6.2.1.4.4 Mechanical anchorage to secure the FRP

If the FRP end is secured by a mechanical anchorage system, confirmation by testing should be considered, so that anchorages have properties which comply with design assumptions. The mechanical anchorage increases the resisting FRP force by ΔF_{ad} , hence Eq.(6-34) may be written as

$$F_{aa} = b_f \cdot t_f \cdot a(s_r) + \Delta F_{ad} \quad (6-35)$$

Depending on the efficiency of the anchorage system, the resisting FRP force may reach the tensile strength of the material. As a more conservative approach, the stress in the FRP shall be limited to 0.9f

6.2.1.5 Localised strengthening

In cases where strengthening is done in a small region of the member (localised strengthening), the FRP may only be subjected to a force that can be anchored at an individual crack and is thus less utilised.

For localised strengthening, the bond length on both sides of the region requiring strengthening shall be equal to at least the member height plus the maximum anchorage length l (Fig.6-6). The tensile force carried by the FRP reinforcement at the cracked area where localised strengthening has been applied is equal to the maximum bond force F_d calculated as follows:

$$F_{fibd} = b_f \cdot t_f \frac{f_{fibk}}{\gamma_{fb}} \quad (6-36)$$

If the FRP is secured by mechanical anchorage, the provisions of Section 6.2.1.3.4 apply.

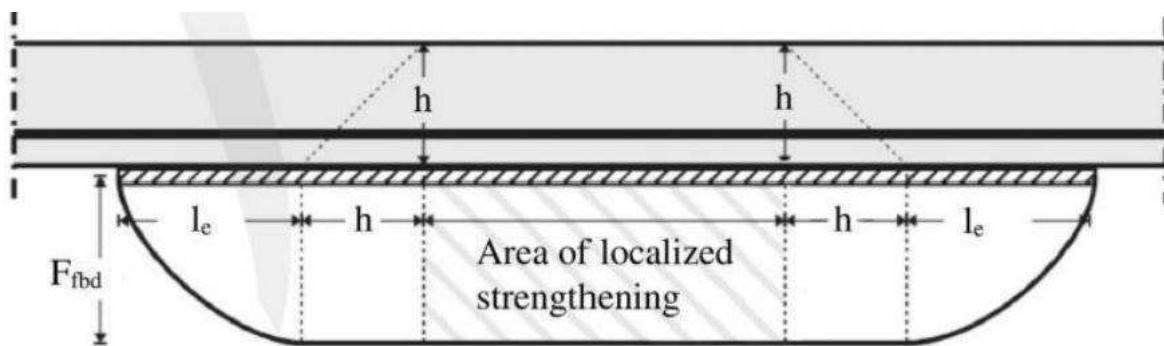


Fig.6-6 Externally bonded FRP for localised strengthening

6.2.2 Flexural strengthening with near surface mounted strips

6.2.2.1 Basic principles

The design of NSM is conducted following the same principles as for EBR. First, the proof of flexural capacity in accordance with Section 6.2.2.2 and an end debonding analysis in accordance with Section 6.2.2.3 shall be conducted. Next, a shear resistance analysis (Section 6.3.4) and an analysis to prevent concrete cover separation (Section 6.3.5) shall be carried out. As in the case of externally bonded FRP, yielding of the internal steel reinforcement should develop prior to failure of FRP or concrete in the compression zone. If the flexural strengthening is to be designed for predominantly non-static actions, a fatigue analysis according to Section 6.8 shall be conducted. Anchorage by transverse FRP or mechanical fasteners may be required if load reversals are expected.

6.2.2.2 Analysis of flexural capacity

The strain in the FRP strip shall not exceed $\varepsilon_{frd,max}$, given as follows:

$$\varepsilon_{frd,max} = \eta \frac{f_{ik}}{\gamma_f \cdot E_f} = \frac{f_{id}}{E_f} \quad (6-37)$$

with these parameters as defined in Section 3.6.2, considering $\eta=0.8$. The effective depth d_f of the FRP is calculated as (Fig. 6-7):

$$d_f = h - \left(t_s - \frac{b_f}{2} \right) \quad (6-38)$$

where t_s = depth of the groove.

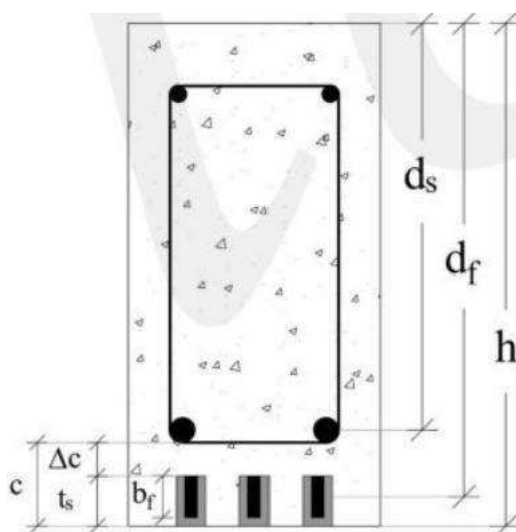


Fig. 6-7 Geometry of cross section with NSM reinforcement

The maximum tensile force carried by the FRP equals

$$FRd = fA \quad (6-39)$$

The state of strain in the cross section at the time of strengthening may be determined assuming that the cross section is cracked.

The cross-sectional analysis is conducted as outlined in Appendix 6.1. At each cross section of the strengthened member, it shall be ensured that the design resistance of the member is higher than the design value following from the applied load. Hereby, the full contribution of the NSM reinforcement can be assumed, up to the strain level given in Eq.(6-37), without further verification of intermediate crack debonding. Debonding near the NSM end zones is verified according to the next section.

6.2.2.3 Analysis of ultimate bond strength, curtailment of longitudinal tension reinforcement

The curtailment of longitudinal NSM tension reinforcement in the ultimate limit state shall be assessed in a similar approach as in Section 6.2.1.4.1, assuming a fully cracked state (Fig.6-8). The tensile force envelope is obtained by taking into account the shift rule, according to Sections 9.2.1.3 for beams or 9.3.1.1 for slabs of EN 1992-1-18. Different strains of the individual reinforcement layers and grading of reinforcing steel cross sections shall be taken into account. The tensile force in the FRP that can be anchored, along the bond length, through bond between the FRP and the concrete, F_{bd} , shall be obtained as discussed in Section 5.5. A tentative proposal is given by means of Eqs(6-40)-(6-41) (DAfStb 20124):

$$F_{bd} = 0.95b_r \cdot \tau_{bd} \sqrt{a_r l_b} (0.4 - 0.0015l_b) \quad \text{for } l_b \leq 115 \text{ mm} \quad (6-40)$$

$$F_{bd} = 0.95b_r \cdot \tau_{bd} \sqrt{a_r} \left[26.2 + 0.065 \tanh\left(\frac{a_r}{70}\right) (l_b - 115) \right] \quad \text{for } l_b > 115 \text{ mm} \quad (6-41)$$

where F_d =design bond load capacity per strip in N, l_b =anchorage length of the strip (Fig.6-8) in mm, τ_{bd} =design bond strength in MPa, b =width of FRP strip in mm and a_r =distance from the longitudinal axis of the strip to the free edge in mm (not to be taken more than 150 mm in the calculation).

Determination of tensile forces in steel and FRP|(example)

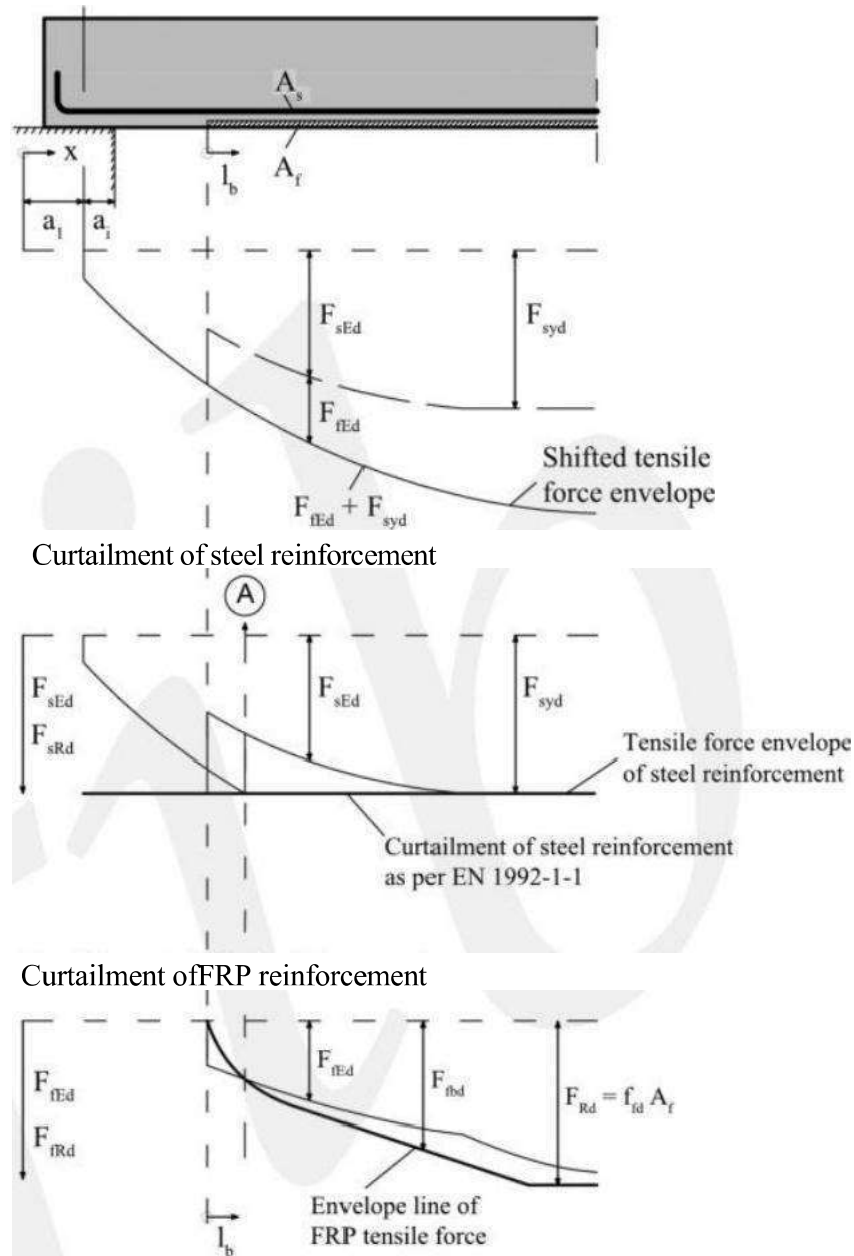


Fig.6-8 End debonding analysis for NSM strips⁴

The design bond strength of NSM FRP strips can be obtained from the minimum bond strength of concrete and adhesive:

$$\tau_{b1d} = \frac{1}{\gamma_{fb}} \min(a_{ba} \cdot \tau_{bak}, a_{bc} \cdot \tau_{bck}) \quad (6-42)$$

where a =product specific factor for long-term behaviour of the adhesive in accordance with testing approvals(=0.5 for pre-dimensioning), abc =product specific factor for long-term behaviour of the concrete in accordance with testing approvals(=0.9 for pre-

Laps of externally bonded reinforcement shall be avoided; they are absolutely not necessary, because FRP can be delivered into the required length. Nevertheless, if needed, lap joints should be made in the direction of the fibres with an overlap that will ensure tensile fracture of the FRP prior to debonding at the lap joint.

6.8 Fatigue

6.8.1 General

Fatigue damage has been shown not to be significant if the FRP-strengthened RC member is exposed to typical service load ranges (between 30% and 60% of the load required to induce first yield), but damage can occur if the load range exceeds 60% of the load at first yield²³. For that reason, care is advised in designing FRP strengthening when the new service loads are significantly higher than they were for the original structure. In such cases, for both FRP-strengthened and unstrengthened beams under fatigue loading, tests show that failure most commonly occurs by fracture of the main steel reinforcement in peak moment zones.

FRP materials themselves possess excellent fatigue resistance, so fatigue failure of the FRP prior to that of the embedded steel has practically not been observed in tests. However, the FRP-to-concrete bond underpins the composite action that leads to the reduction of stress within the steel reinforcement. Local loss of FRP-concrete bond initiated at positions of peak moment (e.g. at crack positions) may lead to higher stresses in the steel reinforcement as the number of cycles increases, hence fatigue of the bond should be taken into account.

6.8.2 Verification conditions

A fatigue analysis under predominantly non-static action shall be conducted for the adhesive bond and for all strength mechanisms that depend on the tensile strength of concrete. As stated in Section 5.3.4 for EBR and in Section 5.5.3 for NSM, given the existing limits for the stress amplitude of internal steel reinforcement and given that the bond strength is not affected by fatigue for typical service load levels below 60% of the yield load, the bond performance of the applied FRP can be regarded not critical for most situations. In the event of concerns, for externally bonded reinforcement an analysis can be conducted in accordance with Section 6.8.3 and for NSM reinforcement in accordance with Section 6.8.4.

In addition to the fatigue analysis for the bonded reinforcement, a fatigue analysis in accordance with EN 1992-1-1⁸ shall be conducted for the concrete, the reinforcing steel and the prestressing steel. This analysis applies to steels in accordance with EN 1992-1-18 Sections 3.2 and 3.3. Additional tests will be required for other/older steels that already exist in the member to be strengthened.

6.8.3 Externally bonded reinforcement

According to DAfStb⁴, forces in the externally bonded reinforcement under predominantly non-static action shall be determined at each element between cracks and at the anchorage. A fatigue analysis shall be conducted at the respective element between cracks and at the anchorage. An analysis of the strip force difference to be anchored shall be conducted in accordance with Section 6.8.3.1. If this analysis cannot be conducted, the stress range of the strip force to be anchored shall be furnished in

accordance with Section 6.8.3.2. The strip forces may be obtained assuming a uniform strain state.

6.8.3.1 Analysis of the strip force difference

An analysis of damage due to a stress amplitude may be omitted if it can be demonstrated that the elastic zone according to the bond stress-slip law will not be exceeded under a combination of actions in accordance with EN 1992-1-1, Section 6.8.38. For this, the following condition shall be satisfied⁴:

$$\Delta F_{fRd,fat1} = 0.348 f_{ctm,surf}^{1/4} \cdot \Delta F_{fRd} \geq \Delta F_{fE,eqv} \quad (6-85)$$

where $f_{m,sur}$ =mean tensile surface strength of concrete (in MPa), ΔF_{Rd} =design resistance to strip force difference and $\Delta F_{fE,eqv}$ = strip force difference in accordance with Eq.(6-4) at the respective element between cracks under a combination of actions in accordance with Section 6.8.3(3) of EN 1992-1-18, or strip force under a combination of actions in accordance with Section 6.8.3(3) of EN 1992-1-1⁸, at the flexural crack closest to the point of zero moment, taking into account the shift of the tension envelope.

The design resistance to strip force difference is obtained as follows:

$$\Delta F_{fRd} = \frac{\Delta F_{fk,B}}{\gamma_{fb}} \text{ (kN)} \quad (6-86)$$

where ΔF_{Ag} =base bond strength at an element between cracks in accordance with Eq.(6-11).

6.8.3.2 Analysis of the stress range at the crack edge subjected to a higher load

If the condition in Eq.(6-85) is not satisfied, the following analysis under the combination of actions in accordance with EN 1992-1-18, Section 6.8.3 shall be conducted⁴:

$$\Delta F_{fRd,fat2} \geq \Delta F_{fEd,fat} \quad (6-87)$$

where the analysis of the stress range resistance at the crack edge ΔF_{Rdfan} shall be obtained as follows:

$$\Delta F_{fRd,fat2} = \alpha \cdot \Delta F_{fRd} \quad (6-88)$$

where: ΔF_{Rd} =design resistance to strip force difference in accordance with Eq.(6-86)(for the strip force at the crack edge subject to the lowest load, the higher load F_d shall be used); α =reduction factor = $-c(\Delta F_{fEd}^U / \Delta F_{fRd}) + c$; c =factor taking into account the stress cycles=0.342(N/N)*1/k; N=number of stress cycles of the action; N*=reference value of stress cycles = $2 \cdot 10^6$; k=23.2 for $N \leq N^*$ or 45.4 for $N \geq N^*$.

The design stress range due to the applied strip forces at the crack edge ΔF_d , a subjected to the higher load shall be obtained as follows:

$$\Delta F_{fEd,fat} = \Delta F_{fEd}^H - \Delta F_{fEd}^L \quad (6-89)$$

where: ΔF_{fEd}^H = strip force difference ΔF , under higher load and cyclic action in accordance with Section 6.8.3(3) of EN 1992-1-18, at the respective element between cracks, or strip force under cyclic action in accordance with Section 6.8.3(3) of EN 1992-1-18, at the flexural crack closest to the point of zero moment, taking into account the shift of the tension envelope; and ΔF_{fEd}^L = strip force difference ΔF , under lower load and non-cyclic action in accordance with EN 1992-1-1, Section 6.8.3(2), at the respective element between cracks or strip force under

non-cyclic action in accordance with Section 6.8.3(2) of EN 1992-1-18, at the flexural crack closest to the point of zero moment, taking into account the shift of the tension envelope.

6.8.4 Near surface mounted reinforcement

With up to $2 \cdot 10^6$ stress cycles, sufficient resistance to fatigue of NSM reinforcement may be assumed, if, under frequent cyclic action according to Section 6.8.3(3) of EN 1992-1-18, the anchorage force taking into account the shift of the tension envelope does not exceed $0.6 F_{b,Rd}$ and the strip stress range $\Delta \sigma$, does not exceed⁴

$$\Delta \sigma_f \leq \frac{500 \text{ N/mm}^2}{t_f} \text{ (MPa)} \quad (6-90)$$

where the strip thickness t_f is in mm.

As a simplification of the above approach, the analysis may be conducted using a frequent combination of actions in accordance with EN 1992-1-1, Section 6.8.6.8. If this analysis can be conducted, no further tests will be necessary.

Design methods for stress cycles greater than $2 \cdot 10^6$ are not covered.

Appendix 6.1 Cross section analysis at the ultimate limit state

The design bending moment of the strengthened cross section is calculated based on principles of RC design (Fig.A6.1-1). First, the neutral axis depth is calculated from strain compatibility and internal force equilibrium, and then the design moment is obtained by moment equilibrium.

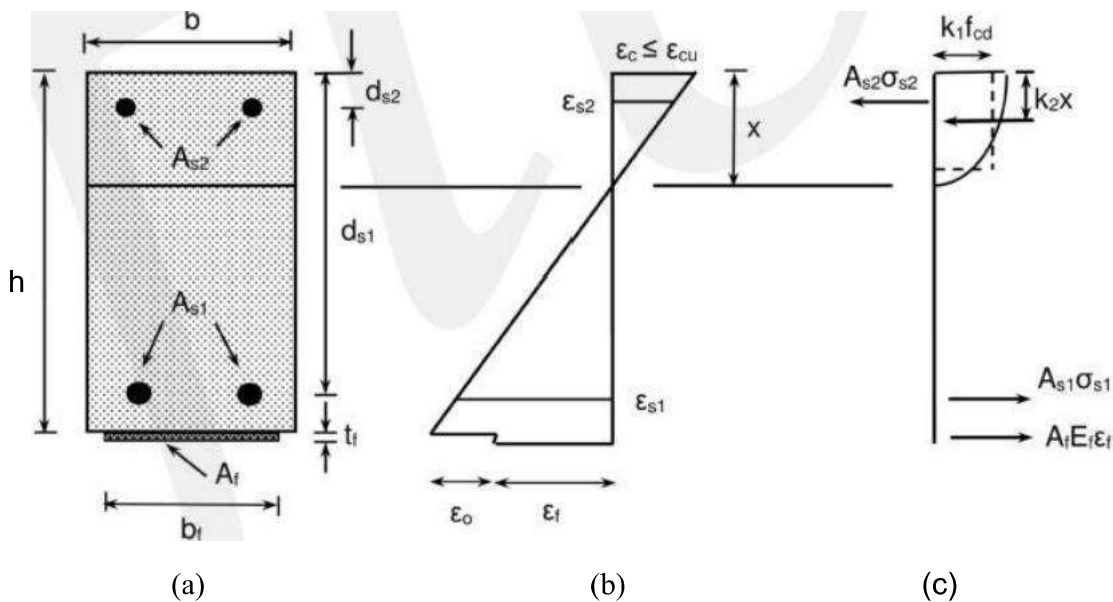


Fig.A6.1-1 Cross section analysis:(a)Geometry,(b)strain distribution,(c)internal forces

The equilibrium of internal forces (Fig.A6.1-1) gives:

$$k_1 f \cdot b \cdot x + A_s2 \sigma_s2 = A_s1 \sigma_s1 + A_f E_f \varepsilon_f \quad (A6-1)$$

The flexural resistance of the cross section is:

$$M = A_s \cdot o \cdot (d - k_2 \cdot x) + A_s \cdot E_s \cdot e_s \cdot (h - k_2 \cdot x) + A_s \cdot \textcircled{2} \cdot 2(k_2 \cdot x - d_{s2}) \quad (\text{A6-2})$$

The stresses in the steel reinforcement are calculated as follows:

$$\sigma_{s1} = \min\left(\varepsilon_c \frac{d_{s1} - x}{x}, \frac{f_yd}{E_s}\right) E_s \quad (\text{A6-3})$$

$$\sigma_{s2} = \min\left(\varepsilon_c \frac{x - d_{s2}}{x}, \frac{f_yd}{E_s}\right) E_s \quad (\text{A6-4})$$

The strain in the FRP is

$$\varepsilon_f = \varepsilon_c \frac{h - x}{x} - \varepsilon_0 \quad (\text{A6-5})$$

where ε_0 = prestrain, i.e. strain in the extreme tension fibre of the cross section during strengthening. Based on the theory of elasticity and with M_o the service moment (no load safety factors are applied) acting on the critical RC section during strengthening, the strain distribution of the member, and hence ε_0 , can be evaluated. For detailed provisions reference is made to fib 2001 Externally Bonded FRP Reinforcement for RC Structures (Section 4.2). As M_o is typically larger than the cracking moment, the calculation is based on a cracked section. If M_o is smaller than the cracking moment, ε_0 can be neglected.

Finally, the factors k_1 and k_2 for the average compressive stress and the lever arm of the parabolic-rectangular stress distribution of concrete are determined as a function of the maximum compressive concrete strain ε as follows:

$$k_1 = \begin{cases} 1000\varepsilon_c \left(0.5 - \frac{1000}{12}\varepsilon_c\right) & \text{for } \varepsilon \leq 0.002 \\ 1 - \frac{2}{3000\varepsilon_c} & \text{for } 0.002 \leq \varepsilon \leq 0.0035 \end{cases} \quad (\text{A6-6})$$

$$k_2 = \begin{cases} \frac{8 - 1000\varepsilon_c}{4(6 - 1000\varepsilon_c)} & \text{for } \varepsilon \leq 0.002 \\ \frac{1000\varepsilon_c(3000\varepsilon_c - 4) + 2}{2000\varepsilon_c(3000\varepsilon_c - 2)} & \text{for } 0.002 \leq \varepsilon \leq 0.0035 \end{cases} \quad (\text{A6-7})$$

Appendix 6.2 Verification of debonding at intermediate cracks according to the moment-shear interaction diagram approach

This approach^{24,25} is based on a bending moment - shear force interaction diagram related to intermediate crack (IC) debonding, obtained through the limit force variation ΔF (see the simplified analysis in Section 6.2.1.2.2). The interaction diagram (Fig. A6.2-1) is obtained by calculating the shear force and bending moment values associated with the maximum transferred force along the crack spacing for some key points related to steel yielding in the critical cracks involved. The method directly compares the design shear force and bending moment values with the IC debonding interaction diagram. If the design values are under the

interaction diagram, IC debonding will not occur. However, the disadvantage of evaluating the crack spacing still remains in this approach.

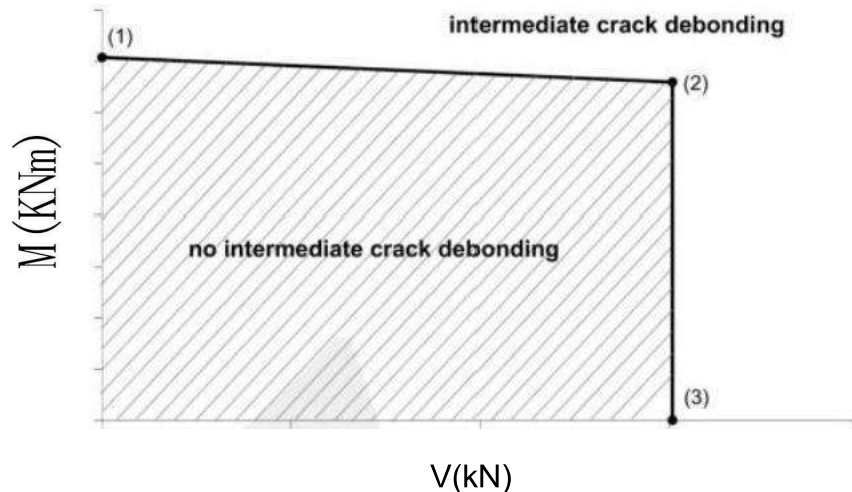


Fig.A6.2-1:Bending-shear interaction diagram for intermediate crack debonding

The interaction diagram is defined as follows:

$$v(1)=0 \quad (\text{A6-8})$$

$$M^{(1)} = M_y + V^* \left(s_r + \frac{V^* \cdot s_r}{V^{(2)} - V^*} \right) \quad (\text{A6-9})$$

$$V^{(2)} = \frac{P_{\max} \cdot z_f - (M_y - f_y \cdot A_s \cdot z_s) \left[1 - \cos \left(\frac{\pi l_b}{2l_e} \right) \right]}{s_r \cdot \cos \left(\frac{\pi l_b}{2l_e} \right) \left(1 - \frac{f_y \cdot A_s \cdot z_s}{M_y} \right)} - q \frac{s_r}{2} \quad (\text{A6-10})$$

$$M^2) = M \quad (\text{A6-11})$$

$$v(3) = v(2) \quad (\text{A6-12})$$

$$M^3 = 0 \quad (\text{A6-13})$$

where

$$V^* = \frac{1}{s_r} \left\{ P_{\max} \cdot z_f - (M_y - f_y \cdot A_s \cdot z_s) \left[1 - \cos \left(\frac{\pi l_b}{2l_e} \right) \right] \right\} - q \frac{s_r}{2} \quad (\text{A6-14})$$

M is the yield moment of the FRP-strengthened RC section; s_r is the mean crack spacing; P_{\max} is the maximum transferred force according to Eq.(5-8b) in an equivalent pure shear specimen with length l , with l the minimum of the crack spacing s , and the limit value s_m given by Eq.(A6-15) for point(2) or by Eq.(A6-16) when calculating V^* ; f_y is the yield stress of steel; z_s and z_f is the steel and FRP lever arm, respectively; l_b is the effective bond length, which may be estimated from Eq.(5-7a) for the mean value and from Eq.(5-7b) for the characteristic value; and q is the uniform load acting along the crack spacing.

$$s_{r,lim}^{(2)} = 0.637 l_e \cdot \arcsin \left(\frac{P_{\max|\beta_i=1}}{M_y - f_y \cdot A_s \cdot z_s} z_f \right) \quad (\text{A6-15})$$

$$s_{r,lim}^{(*)} = 0.637 l_e \cdot \arctan \left(\frac{P_{\max|\beta_i=1}}{M_y - f_y \cdot A_s \cdot z_s} z_f \right) \quad (\text{A6-16})$$

The term $s_{r,lim}^{(2)}$ refers to point (2) of the interaction diagram and, thus, Eq.(A6-15) has to be introduced in Eq.(A6-10) for calculating l_6 . In analogy, $s_{r,lim}^{(*)}$ refers to point (1) of the interaction diagram and, thus, Eq.(A6-16) has to be introduced in Eq.(A6-14) for calculating l_6 .

Figure A6.2-2 gives the experimental values of the shear strength at debonding along with the mean and the 5% characteristic provisions, assuming a mean value of E/t , equal to 130'000 N/mm and a mean cross section depth of 200 mm, according to an assembled experimental database. A design provision is also plotted, by dividing the 5% characteristic values by 1.5. Mean and characteristic values in the figure were calculated by applying Eq.(6-20) without the safety factor and with values for the other parameters as explained in Section 6.2.1.2.2 (simplified analysis).

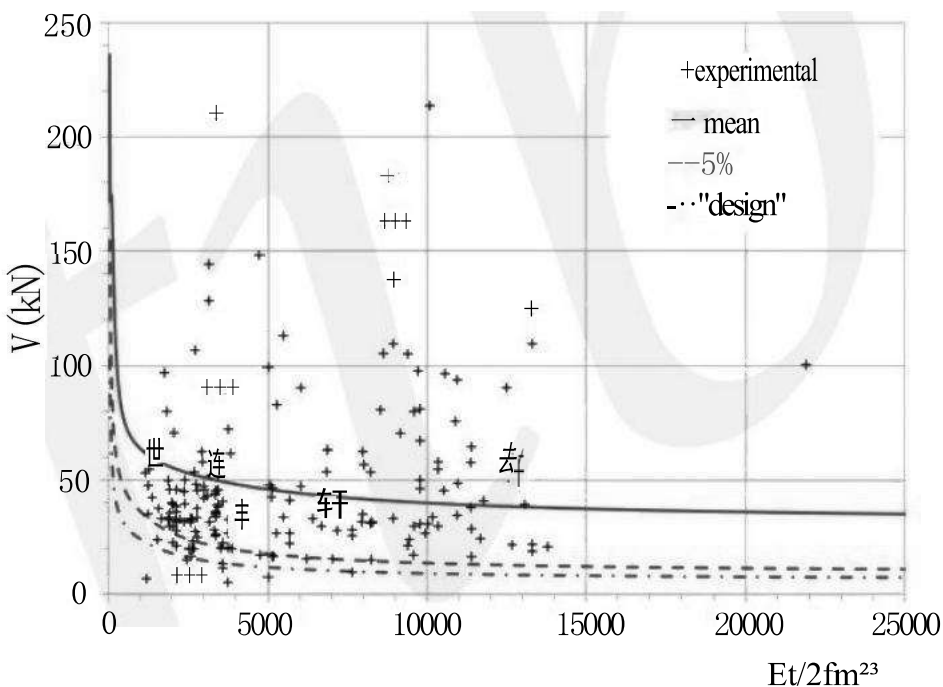


Fig.A6.2-2 Experimental values and theoretical provisions for the maximum shear force at intermediate crack debonding in EBR systems

Appendix 6.3 Verification of debonding at intermediate cracks according to the shear transfer between concrete and FRP approach

This approach implies the limitation of the interfacial shear stress resulting from the change of tensile force along the FRP reinforcement²⁶, assuming a fully cracked state and without explicitly taking into account the position of the flexural cracks. As the FRP tensile force gradient is proportional to the acting shear force V_{Ed} , the acting interface bond strength

can be expressed as given in the right-hand part of Eqs.A6-17a and b. At the ultimate limit state, this interface bond shear stress should be restricted to the design bond shear strength. For this design shear strength several equations have been proposed^{26,27}.

Depending on whether the internal steel has yielded or not, the verification can be simplified as follows:

$$\frac{V_{Ed}}{0.95d_s \cdot b_f \left(1 + \frac{A_s E_s}{A_f E_f} \right)} \leq \tau_{Rd} \quad \text{if } e_s < Ed \quad (\text{A6-17a})$$

$$\frac{V_{Ed}}{0.95d_s \cdot b_f} \leq \tau_{Rd} \quad \text{if } e_s \geq \epsilon \quad (\text{A6-17b})$$

where A_s , E_s , d_s and e are the area, the elastic modulus, the effective depth and the strain of the internal tension reinforcement, respectively, b , A , and E , are the width, the area and the elastic modulus of the FRP reinforcement, respectively and ed is the design yield strain of steel. The design shear strength is calculated as:

$$\tau_{Rd} = \frac{0.23\tau_{b1k} + 0.45\tau_{bfk} + \frac{92.8}{h}}{\gamma_{ib}} \quad (\text{A6-18})$$

where τ_{b1k} is the characteristic value of the bond strength and τ_{bfk} is the characteristic value of the friction term of the bond strength.

Equation(A6-17)is based on the assumption that the design shear force can be obtained from the increase of the bending moment between two sections distant Δx ,and that the total tensile force, N_d ,in both the external FRP and the internal steel reinforcement,is calculated on the basis of a lever arm equal to 0.95d:

$$V_{Ed} = \frac{\Delta M_{Ed}}{\Delta x} \quad N_{Ed} = \frac{M_{Ed}}{0.95d_s} \quad (\text{A6-19})$$

The required storey stiffness K of the retrofitted structure that comprises RC jacketed columns, I_w RC walls, I_x spans of X-brace metallic pairs, I_{mw} masonry walls and I_{cf} columns strengthened with longitudinal FRP strips (EBR or NSM) is equal to:

$$K_i = \sum_{j=1}^{t_{RC}} K_j^i + \sum_{j=1}^{t_w} K_j^w + \sum_{j=1}^{t_x} K_j^x + \sum_{j=1}^{t_{mw}} K_j^{mw} + \sum_{j=1}^{t_{cf}} K_j^f \quad (8-2)$$

The contributions of each of these techniques/elements to the storey stiffness, K , are listed in a study^{6,7} and are summarised here for completeness in Appendix 8.1. Only the possible contribution of FRP to the stiffness terms, K_j^f , is considered in the following detailing paragraphs in the main body of the chapter.

In Eq.(8-2), variables t_{RC}, t_w, t_x, t_{mw} and t_{cf} are defined as follows: t_{RC} is the number of columns retrofitted with RC jackets in a single storey; t_w is the number of RC walls added for stiffening the structure in the direction of action; t_x is the number of X-brace pairs added in the storey to add stiffness-in the direction of action; t_{mw} is the number of infill masonry panels added in the storey in the direction of action; and t_{cf} is the number of columns strengthened with longitudinal FRP strips (externally bonded or NSM).

8.2 Practical implementation of global measures

From the preceding discussion it follows that in practical implementation the displacement demand and the pattern of its distribution may be essential prerequisites to the application of externally applied FRP for seismic retrofitting. Steps in this direction are the following⁵: (1)determine if a global intervention is required,(2)target for an improved period estimate, (3)target for an improved shape of the fundamental mode, and (4)determine the required stiffness. Detailed considerations on these prerequisite steps are given in Appendix 8.2.

8.3 Strategies in FRP interventions for seismic applications

Seismic retrofitting of RC structures with FRP may be used in order to upgrade a variety of structural deficiencies, if upon assessment according to the established code framework (EN 1998-3:2005)⁸ it is shown that seismic safety may be compromised at the design performance limit state. Both for evaluating the structure's safety and in defining the retrofit objectives, reference is made to verification of acceptable limit states as described in the reference code document.

Similarly, the seismic hazard considered for the retrofit is identical to that used for new designs, unless the National Standards enable through special provisions, assigning a different importance level category to the retrofitted structure so as to account for a residual service life different from the 50-year standard.

Analysis of the retrofitted structure may be used to check against the established acceptance criteria, following the methods of analysis used in the assessment procedure.

Material safety factors refer to FRP materials typically used today (e.g. GFRP, CFRP and AFRP with strengths ranging from 1500 to 3500 MPa and nominal rupture strains from 2.5% down to 1.5%). For retrofit design these are: (a) For existing concrete and steel reinforcement, the confidence factors are used to divide mean material strength values depending on the knowledge level attained (EN 1998-3:2005)⁸. (b) For FRP: The material safety factor depends on the application method of the FRP material and the member classification,